

Cite this: *J. Mater. Chem.*, 2012, **22**, 23655

www.rsc.org/materials

PAPER

## Polymer photovoltaic wires based on aligned carbon nanotube fibers†

Tao Chen, Longbin Qiu, Houpu Li and Huisheng Peng\*

Received 2nd August 2012, Accepted 24th September 2012

DOI: 10.1039/c2jm35158g

Compared with the conventional planar structure, a wire-shaped polymer solar cell which is weavable exhibits unique and promising applications. However, it is rare to realize such a useful structure in polymer solar cells due to the difficulty in finding appropriate electrodes. Herein, we have fabricated polymer photovoltaic wires by using aligned carbon nanotube fibers as electrodes. The high flexibility, high electrical conductivity, and elaborate nanostructure of the nanotube fiber electrode enables an effective charge separation and transport. The resulting wire cell showed an open-circuit voltage, short-circuit current density and fill factor of 0.42 V, 0.98 mA cm<sup>-2</sup> and 0.36, respectively, which produce an energy conversion efficiency of 0.15%.

## Introduction

Organic photovoltaic wire has recently attracted increasing interest due to the unique advantage of being weavable compared with a conventional planar structure.<sup>1–5</sup> In the case of a wire structure, dye-sensitized solar cells have been widely explored, while polymer solar cells are rare although they can be more conveniently fabricated through a solution process without the use of a liquid electrolyte in the device, which enables a higher stability during the use.<sup>1–7</sup> This fact may be explained by the different requirements in electrodes. A wire cell is typically made by twining two wire electrodes, such as metal wires or polymer fibers coated with conductive layers on the outside. Both of them are relatively rigid with smooth surfaces, which are fine for dye-sensitized solar cells due to the use of a liquid electrolyte. However, it remains challenging for polymer photovoltaic wires as the resulting ineffective interface between the two rigid wire electrodes can not provide an effective charge separation and transport. Therefore, new electrodes with a high flexibility and elaborate surface are urgently required to produce polymer photovoltaic wires.

Recently, aligned carbon nanotube (CNT) fibers have been widely investigated due to their combined excellent properties, such as light weight, good flexibility, high electrical conductivities, high mechanical strengths and high electrocatalytic activities.<sup>8–13</sup> In addition, the elaborate nanostructure on the surface of CNT fibers can also improve the charge separation and transport. They could be used as either working or counter electrodes, or even as the conductive substrates for both working and counter electrodes in dye-sensitized solar cells.<sup>3,12</sup>

On the other hand, an interpenetrating network between polymeric donor and fullerene acceptor was generally designed to enhance the charge separation and transport due to a high interfacial area in polymer photovoltaics.<sup>14,15</sup> Although this structure can decrease the diffusion distance of excitons toward the heterojunction interface to reduce the free charge recombination, a large efficiency loss resulted from inefficient charge transport in the active polymer layer with a disordered bulk heterojunction structure.<sup>15</sup> Therefore, a lot of efforts have been made to increase the charge transport ability by optimizing the morphology of donor–acceptor interfaces, *e.g.*, aligned semi-conductive nanotubes, nanorods and nanowires including titanium dioxide and zinc oxide were introduced to the hybrid organic–inorganic photoactive layer.<sup>16–19</sup>

Herein, aligned CNT fibers have been developed as electrodes to fabricate polymer photovoltaic wires. Fig. 1a and b schematically show the structure of a typical wire cell in which a CNT fiber is twined with a TiO<sub>2</sub> nanotube-modified Ti wire where poly(3-hexyl-2,5-thiophene) (P3HT) and (6,6)-phenyl-C<sub>71</sub> butyric acid methyl ester (PC<sub>70</sub>BM) are used as photoactive

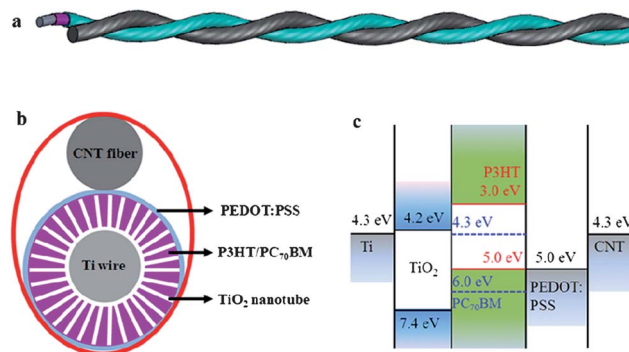


Fig. 1 (a) and (b) Schematic illustration of a polymer photovoltaic wire from side and top views, respectively. (c) Energy level diagram.

State Key Laboratory of Molecular Engineering of Polymers, Department of Macromolecular Science, Laboratory of Advanced Materials, Fudan University, Shanghai 200438, China. E-mail: penghs@fudan.edu.cn

† Electronic supplementary information (ESI) available. See DOI: 10.1039/c2jm35158g

materials. The energy level diagram is shown in Fig. 1c. The energy level of  $\sim 4.3$  eV for CNTs is close to the conventional aluminum electrode and makes the fiber an effective electrode.  $\text{TiO}_2$  has been also introduced to enhance the charge separation and electron transport as the conduction band of 4.2 eV is located between the lowest unoccupied molecular orbital of P3HT and the energy level of Ti. The generation of electric power is summarized as below: (1) P3HT generates excitons after the adsorption of sunlight; (2) the excitons are separated into electrons and holes at the interface of P3HT/ $\text{PC}_{70}\text{BM}$  or P3HT/ $\text{TiO}_2$ ; (3) the electrons are transported through  $\text{PC}_{70}\text{BM}$  or  $\text{TiO}_2$  and collected by the Ti wire, while the holes are transported along the conjugated backbone of P3HT and collected by the CNT fiber after they transport across the layer of poly(3,4-ethylenedioxythiophene) and poly(styrenesulfonate).

## Experimental section

CNT arrays were synthesized by chemical vapor deposition in a quartz tube furnace at  $740^\circ\text{C}$ , in which Fe (1.2 nm)/ $\text{Al}_2\text{O}_3$  (3 nm) on a silicon wafer was used as the catalyst, ethylene was used as the carbon source with a flow rate of 90 sccm, and a mixture of Ar (400 sccm) and  $\text{H}_2$  (30 sccm) was used as carrier gas. CNT fibers were then spun from the array by using a microprobe with a rotary speed of 2000 revolutions per minute.

Highly aligned titania nanotube arrays grown on titanium wires were formed by an electrochemical anodic oxidation method in 0.25 wt%  $\text{NH}_4\text{F}$ /ethylene glycol solution containing 5 vol%  $\text{H}_2\text{O}$  at 60 V over different times. The growth was realized in a two-electrode electrochemical cell with a titanium wire (diameter of 127  $\mu\text{m}$  and purity of 99.9%) and Pt plate as the anode and cathode, respectively. After being washed by deionized water, the resulting wires were annealed at  $500^\circ\text{C}$  in air for 1 h to produce the anatase titania. As a comparison, a layer of titanium dioxide nanoparticles was coated onto a Ti wire by dipping it into a  $\text{TiO}_2$  colloid (TPP3, purchased from Dalian Heptachroma Solartech Co., Ltd.), followed by evaporation of the solvent under heating at  $100^\circ\text{C}$  for 5 min. The resulting titanium dioxide nanoparticle-coated Ti wire was finally sintered at  $500^\circ\text{C}$  for 60 min in air.

For the fabrication of the polymer photovoltaic wires, a typical process is summarized as below. After the temperature was decreased to  $120^\circ\text{C}$ , the annealed Ti wire with a titania nanotube array was immersed into a mixed solution of P3HT (from Solarmer Co., Ltd. Beijing) ( $10\text{ mg mL}^{-1}$ ) and  $\text{PC}_{70}\text{BM}$  (from Solarmer Co., Ltd. Beijing) ( $8\text{ mg mL}^{-1}$ ) in *o*-dichlorobenzene for 2 h at room temperature. The treated wire was taken out to evaporate the solvent in air. A layer of PEDOT:PSS was then coated on the outer surface through a dip-coating process in a PEDOT:PSS aqueous solution (5 wt%) (from Bayer Co., Ltd.) with 5 vol% of dimethylsulfoxide. The polymer photovoltaic wire was finally fabricated by twining the above modified Ti wire and a CNT fiber. The two electrodes were fixed on a piece of glass using indium by an ultrasonic soldering mate (USM-V, Kuroda Techno Co., Ltd.). At least six samples were fabricated in any case, and all devices were directly made in air.

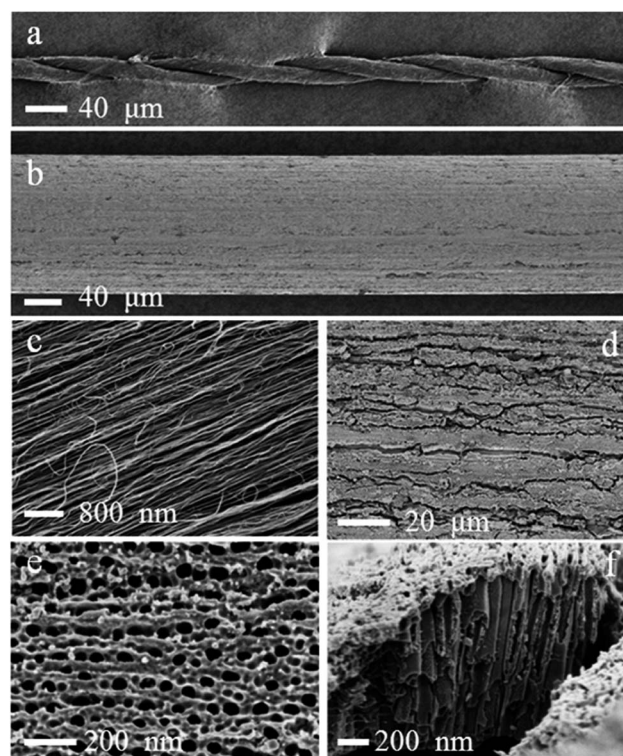
The structures were characterized by SEM (Hitachi FE-SEM S-4800 operated at 1 kV) and TEM (JEOL JEM-2100F operated at 200 kV). Stress–strain curves were obtained from a Shimadzu

Table-Top Universal Testing Instrument. A CNT fiber was mounted on a paper tab with a gauge length of 5 mm, and the fiber diameter was measured by SEM. The cell was measured by recording  $I$ – $V$  curves with a Keithley 2400 Source Meter under illumination ( $100\text{ mW cm}^{-2}$ ) of simulated AM 1.5 solar light coming from a solar simulator (Oriel-Sol3A 94023A equipped with a 450 W Xe lamp and an AM 1.5 filter). The light intensity was calibrated using a reference Si solar cell (Oriel-91150).

## Results and discussion

CNT fibers were prepared from CNT arrays by a dry-spinning process,<sup>11–13</sup> and they were uniform in both diameter and structure as shown by the scanning electron microscopy (SEM) images (Fig. 2a and S1†). Multi-walled CNTs had been used, and they were highly aligned to provide the fiber with excellent properties (Fig. 2c).<sup>11,12</sup> For instance, the CNT fiber was flexible and could be closely and stably twisted with another CNT fiber (Fig. 2a) or other fiber materials. In addition, it exhibited a tensile strength of  $\sim 600\text{ MPa}$  (shown in Fig. S2†) and electrical conductivity of  $10^3\text{ S cm}^{-1}$ . The CNT fiber also exhibits an elaborate nanostructure on the surface, which can improve the charge separation and transport. The combined excellent properties and unique structure make the CNT fiber an ideal electrode candidate.

Here, aligned  $\text{TiO}_2$  nanotubes were designed to increase the charge transport capability, and they were grown on a Ti wire by electrochemical anodic oxidation.<sup>16–19</sup> The height of the  $\text{TiO}_2$



**Fig. 2** Scanning electron microscopy (SEM) images. (a) Two twisted CNT fibers. (b) A Ti wire after anodizing oxidation for 5 min. (c) A CNT fiber at high magnification. (d) and (e) Higher magnifications of (b). (f) Side view of (b).

nanotube arrays could be controlled from 350 nm to 7  $\mu\text{m}$  by tuning the time of anodic oxidation from 1 to 30 min. The array height plays a critical role in the performance of the polymer photovoltaic wires and will be discussed later. The anodizing oxidation time of 5 min is first investigated. Fig. 2b and d show that the  $\text{TiO}_2$  nanotubes are stably attached on the Ti wire. The diameters of  $\text{TiO}_2$  nanotubes range from 40 to 80 nm (Fig. 2e), and the height of the  $\text{TiO}_2$  nanotube array is calculated as  $\sim 1.7 \mu\text{m}$  from SEM images. Fig. 2f further shows that the  $\text{TiO}_2$  nanotubes are perpendicularly aligned on the Ti wire.

The polymer photovoltaic wire was then assembled by twisting a CNT fiber and a modified Ti wire coated with a photoactive P3HT/PC<sub>70</sub>BM layer. Fig. 3a shows a representative SEM image in the middle part of a wire cell with a uniform structure. Due to the high tensile strength and high flexibility of the CNT fiber, the two fiber electrodes could be tightly twined with a good surface contact (Fig. 3b and c), which was critically important for the effective separation and transport of charges. Fig. 3c further shows that the CNT fiber maintained its structural integrity when it was bent during the twining process. The photovoltaic components were also found to be efficiently infiltrated into the array and uniformly dispersed among the  $\text{TiO}_2$  nanotubes (Fig. 3d and S3†). The polymer photovoltaic wires exhibited a high flexibility and weavability, and could be easily made into a knot (Fig. 3e) or integrated into the other textiles.

The photovoltaic performance of the wire cell was characterized under AM 1.5 illumination (light intensity of  $100 \text{ mW cm}^{-2}$ ). The power conversion efficiency ( $\eta$ ) is calculated by the equation of  $\eta = \text{FF} \times V_{\text{oc}} \times J_{\text{sc}}/P_{\text{in}}$ , where FF,  $V_{\text{oc}}$ ,  $J_{\text{sc}}$  and  $P_{\text{in}}$  represent fill factor, open-circuit voltage, short-circuit current density and incident light power density, respectively. The effective area was obtained by multiplying the length and diameter of the photoactive wire. The values of  $V_{\text{oc}}$ ,  $J_{\text{sc}}$  and FF were obtained as 0.42 V,  $0.98 \text{ mA cm}^{-2}$  and 0.36, respectively, which produced an  $\eta$  of 0.15% (Fig. 4a). As a comparison, if a metal wire such as an aluminum wire (diameter of 28  $\mu\text{m}$ ) was

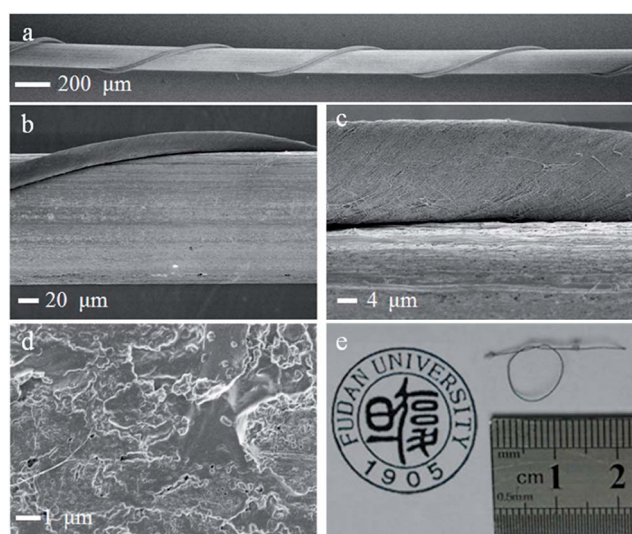


**Fig. 3** (a) SEM image of a middle part of the polymer photovoltaic wire. (b) and (c) Higher magnifications of (a). (d) SEM image of the  $\text{TiO}_2$  nanotube array coated with P3HT:PC<sub>70</sub>BM. (e) Photograph of a wire cell in the format of a knot.

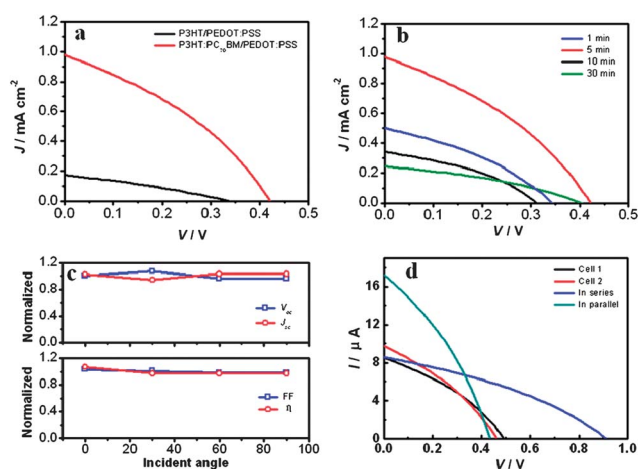


**Fig. 4** (a)  $J$ - $V$  curves of typical polymer photovoltaic wires with and without PC<sub>70</sub>BM. (b)  $J$ - $V$  curves of polymer photovoltaic wires using Ti wires with different anodizing times. (c) Dependence of the photovoltaic parameters on the incident angle. (d)  $I$ - $V$  curves of the two wire cells as well as their connections in series and in parallel.

used in replacement of the CNT fiber, obvious gaps were observed between two electrodes (Fig. S4†), and no photocurrents were produced in the resulting wire cell. To better understand the photovoltaic wire, more control experiments were made. If a thin layer of  $\text{TiO}_2$  nanoparticles was used to replace the nanotubes on the Ti wire (Fig. S5†), a decreasing photocurrent of  $0.03 \text{ mA cm}^{-2}$  was obtained (Fig. S6†). If a Ti wire coated with a thin layer of  $\text{TiO}_2$  film or a bare Ti wire was twined with the CNT fiber (Fig. S7†), almost no photocurrent was generated. These results show that the nanostructured surface on the electrode is critically important for the effective charge separation and transport, while the aligned  $\text{TiO}_2$  nanotubes further increase the cell performance. On the other hand, when no PC<sub>70</sub>BM was used in the photoactive layer,  $V_{\text{oc}}$ ,  $J_{\text{sc}}$ , FF and  $\eta$  were 0.36 V,  $0.17 \text{ mA cm}^{-2}$ , 0.31 and 0.02%, respectively. The introduction of PC<sub>70</sub>BM as the acceptor can efficiently enhance the separation of electron-hole pairs and the transport of electrons, although the  $\text{TiO}_2$  nanotubes may also transport the electrons.

To investigate the dependence of the photovoltaic performance on the thickness of the photoactive layer, Ti wires with different anodizing times were used to fabricate the polymer photovoltaic wires. The heights of the  $\text{TiO}_2$  nanotube arrays were increased from 350 nm to 1.7  $\mu\text{m}$ , 3  $\mu\text{m}$ , and 7  $\mu\text{m}$  (Fig. 5) when the anodizing time was increased from 1 to 5, 10 and 30 min, respectively. Accordingly,  $J_{\text{sc}}$  was first increased from 0.5 to  $0.98 \text{ mA cm}^{-2}$  and then decreased to 0.34 and  $0.24 \text{ mA cm}^{-2}$ , and  $\eta$  was also increased from 0.06% to 0.15% and then decreased to 0.04% and 0.03% (Fig. 4b). This phenomenon can be explained by the different morphologies and lengths of  $\text{TiO}_2$  nanotubes. No uniform tubular structure had been formed during the growth for 1 min (Fig. 5a). Although the height of the  $\text{TiO}_2$  nanotubes was appropriate for a polymer cell, it was difficult for P3HT to be effectively infiltrated and uniformly dispersed, which produced low power conversion efficiencies. On the other hand, when the  $\text{TiO}_2$  nanotube array was equal to or thicker than 3  $\mu\text{m}$  with an anodizing time of 10 min or longer, it became difficult for effective light harvesting, which increased the recombination

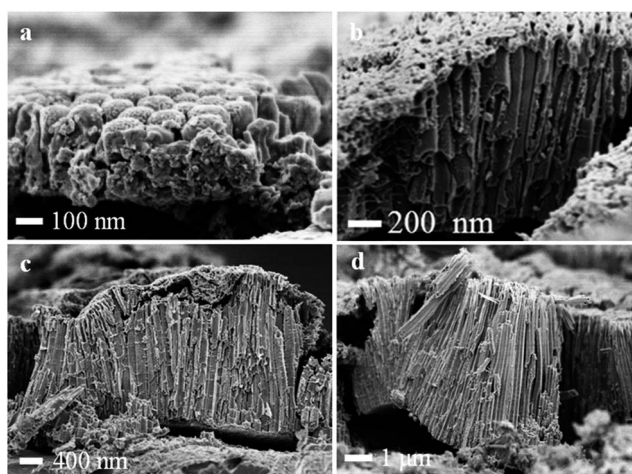


**Fig. 5** SEM images of TiO<sub>2</sub> nanotube arrays being anodized for (a) 1 min, (b) 5 min, (c) 10 min, and (d) 30 min, all as side views.

between electrons and holes and also gave low power conversion efficiencies, although they owned an integrated tubular structure (Fig. 5c and d). The optimal anodizing time was found to be 5 min with a thickness of the TiO<sub>2</sub> nanotube array of  $\sim 1.7 \mu\text{m}$ . The stability of the polymer photovoltaic wires was also studied, and the value of  $\eta$  remained almost unchanged in five days. More efforts are underway to further improve the power conversion efficiency and other performances.

Due to the unique structure, the parameters of the polymer photovoltaic wires remained almost unchanged under different incident angles with the same light intensity (Fig. 4c). Therefore, they can be efficiently used throughout the day. In addition, the output current and voltage can be further tuned to meet various applications by connection in series and in parallel (Fig. 4d), respectively. For instance, two photovoltaic wires with  $V_{\text{oc}}$  of 0.46 and 0.49 V were connected in series to produce a  $V_{\text{oc}}$  of 0.91 V, almost the sum of the two individual cells. Two wire cells with  $I_{\text{sc}}$  of 8.5 and 9.7  $\mu\text{A}$  were connected in parallel to produce an  $I_{\text{sc}}$  of 17.2  $\mu\text{A}$ , almost the sum of the two individual cells.

## Conclusion

In summary, polymer photovoltaic wires have been realized on the basis of spun CNT fibers as the electrode, and a maximum energy conversion efficiency of 0.15% is obtained. Although the cell efficiency is currently low, this work provides an effective route to the development of wire-shaped polymer solar cells.

More efforts will be paid to improve the photovoltaic performance by further increasing the electrical properties of the CNT fiber and tuning the morphology and structure of the titanium dioxide nanotube.

## Acknowledgements

This work was supported by NSFC (20904006, 91027025), MOST (2011CB932503, 2011DFA51330), MOE (NCET-09-0318), STCSM (11520701400) and The Program for Professor of Special Appointment (Eastern Scholar) at Shanghai Institutions of Higher Learning.

## Notes and references

- X. Fan, Z. Chu, F. Wang, C. Zhang, L. Chen, Y. Tang and D. Zou, *Adv. Mater.*, 2008, **20**, 592–595.
- B. Weintraub, Y. Wei and Z. L. Wang, *Angew. Chem., Int. Ed.*, 2009, **48**, 8981–8985.
- T. Chen, L. Qiu, Z. Yang, Z. Wang and H. Peng, *Nano Lett.*, 2012, **12**, 2568–2572.
- D. Zou, D. Wang, Z. Chu, Z. Lv and X. Fan, *Coord. Chem. Rev.*, 2010, **254**, 1169–1178.
- M. R. Lee, R. D. Eckert, K. Forberich, G. Dennler, C. J. Brabec and R. A. Gaudiana, *Science*, 2009, **324**, 232–235.
- B. O'Connor, K. P. Pipe and M. Shtein, *Appl. Phys. Lett.*, 2008, **92**, 193306.
- A. Bedeloglu, A. Demir, Y. Bozkurt and N. S. Sariciftci, *Text. Res. J.*, 2010, **80**, 1065–1074.
- M. Zhang, K. R. Atkinson and R. H. Baughman, *Science*, 2004, **306**, 1358–1361.
- J. Foroughi, G. M. Spinks, G. G. Wallace, J. Y. Oh, M. E. Kozlov, S. L. Fang, T. Mirfakhrai, J. D. W. Madden, M. K. Shin, S. J. Kim and R. H. Baughman, *Science*, 2011, **334**, 494–497.
- H. Peng, X. Sun, F. Cai, X. Chen, Y. Zhu, G. Liao, D. Chen, Q. Li, Y. Lu, Y. Zhu and Q. Jia, *Nat. Nanotechnol.*, 2009, **4**, 738–741.
- T. Chen, Z. Cai, Z. Yang, L. Li, X. Sun, T. Huang, A. Yu, H. G. Kia and H. Peng, *Adv. Mater.*, 2011, **23**, 4620–4625.
- T. Chen, S. Wang, Z. Yang, Q. Feng, X. Sun, L. Li, Z. Wang and H. Peng, *Angew. Chem., Int. Ed.*, 2011, **50**, 1815–1819.
- H. Peng, M. Jain, Q. Li, D. E. Peterson, Y. Zhu and Q. Jia, *J. Am. Chem. Soc.*, 2008, **130**, 1130–1131.
- G. Yu, J. Gao, J. C. Hummelen, F. Wudl and A. J. Heeger, *Science*, 1995, **270**, 1789–1791.
- S. Günes, H. Neugebauer and N. S. Sariciftci, *Chem. Rev.*, 2007, **107**, 1324–1338.
- S. S. Williams, M. J. Hampton, V. Gowrishankar, I.-K. Ding, J. L. Templeton, E. T. Samulski, J. M. DeSimone and M. D. McGehee, *Chem. Mater.*, 2008, **20**, 5229–5234.
- K. Takanezawa, K. Hirota, Q.-S. Wei, K. Tajima and K. Hashimoto, *J. Phys. Chem. C*, 2007, **111**, 7218–7223.
- K. Shankar, G. K. Mor, H. E. Prakasam, O. K. Varghese and C. A. Grimes, *Langmuir*, 2007, **23**, 12445–12449.
- G. K. Mor, S. Kim, M. Paulose, O. K. Varghese, K. Shankar, J. Basham and C. A. Grimes, *Nano Lett.*, 2009, **9**, 4250–4257.